HHS Public Access

Author manuscript

J Vasc Res. Author manuscript; available in PMC 2022 May 05.

Published in final edited form as:

J Vasc Res. 2021 ; 58(5): 277–285. doi:10.1159/000516044.

Adaptor protein RapGEF1 is required for ERK1/2 signaling in response to elevated phosphate in vascular smooth muscle cells

Nicholas W. Chavkin[1], **Elizabeth M. Leaf**[1], **Kadin E. Brooks**[1], **Mary C. Wallingford**[1], **Susan M. Lund**[1], **Cecilia M. Giachelli**[1]

[1]Department of Bioengineering, University of Washington, Seattle WA USA

Abstract

The sodium-dependent phosphate transporter, SLC20A1, is required for elevated inorganic phosphate (Pi) induced vascular smooth muscle cell (VSMC) matrix mineralization and phenotype transdifferentiation. Recently, elevated Pi was shown to induce ERK1/2 phosphorylation through SLC20A1 by Pi-uptake independent functions in VSMCs, suggesting a cell signaling response to elevated Pi. Previous studies identified Rap1 guanine nucleotide exchange factor (RapGEF1) as a SLC20A1 interacting protein, and RapGEF1 promotes ERK1/2 phosphorylation through Rap1 activation. In this study, we tested the hypothesis that RapGEF1 is a critical component of the SLC20A1-mediated Pi-induced ERK1/2 phosphorylation pathway. Co-localization of SLC20A1 and RapGEF1, knockdown of RapGEF1 with siRNA, and small molecule inhibitors of Rap1, B-Raf, and Mek1/2 were investigated. SLC20A1 and RapGEF1 were co-localized in peri-membranous structures in vascular smooth muscle cells. Knock-down of RapGEF1 and small molecule inhibitors against Rap1, B-Raf, and Mek1/2 eliminated elevated Pi-induced ERK1/2 phosphorylation. Knock-down of RapGEF1 inhibited SM22α mRNA expression and blocked elevated Pi-induced down-regulation of SM22α mRNA. Together, these data suggest that RapGEF1 is required for SLC20a1-mediated elevated Pi signaling through a Rap1/B-Raf/Mek1/2 cell signaling pathway thereby promoting ERK1/2 phosphorylation and inhibiting SM22α gene expression in VSMCs.

Keywords

Inorganic phosphate; Vascular smooth muscle cells; ERK1/2 signaling; RapGEF1; SLC20A1/PiT1

Corresponding Author: Cecilia M. Giachelli, Ph.D., Professor, Department of Bioengineering, University of Washington, Box 355061, Seattle, WA 98195, USA. Tel: (206) 543-0205 ceci@washington.edu.

Author Contributions Nicholas W. Chavkin wrote the manuscript, was involved in experimental design and data analysis, and performed experiments. Elizabeth M. Leaf contributed to the manuscript text, was involved in experimental design and data analysis, and performed experiments. Kadin E. Brooks, Mary C. Wallingford, and Susan M. Lund were involved in data analysis and performed experiments. Cecilia M. Giachelli was involved in experimental design and data analysis, edited the manuscript and figures, and acquired funding for the experiments.

Statement of Ethics

All animal procedures were approved by the Animal Use and Care Committee at the University of Washington.

Conflict of Interest Statement

The authors do not have any conflicts of interest to disclose.

Introduction

Inorganic phosphate (Pi) is an essential molecule required for almost every cellular function, including membrane stability, nucleic acid polymerization, and enzyme activation. Pi is also a main component of hydroxyapatite crystal in bone mineral [1]. A homeostatic balance of Pi intake through the intestines and Pi excretion through the kidneys maintains Pi homeostasis around 1.0 mM, including hormonal regulation of Pi transporters by FGF-23, Vitamin D, PTH, and Klotho [2, 3]. Dysregulation of Pi homeostasis can lead to severe vascular disease phenotypes including vascular calcification, which is the deposition of hydroxyapatite mineral in vascular soft tissue. Patients with late-stage chronic kidney disease have reduced kidney filtration function that leads to hyperphosphatemia (concentrations greater than 1.46mM Pi) [4–6]. Hyperphosphatemia has been correlated to increased prevalence of arterial medial calcification and a greatly increased risk of cardiovascular morbidity and mortality [4–6]. Arterial medial calcification is due in part to elevated serum Pi, which promotes active mineral deposition by vascular smooth muscle cells (VSMCs), leading to matrix mineralization in the medial layer of arteries [2]. This process is initiated by elevated Pi-induced ERK1/2 phosphorylation that leads to down-regulation of VSMC genes such as smooth muscle 22 alpha (SM22α), consistent with VSMC phenotype change [7, 8]. However, the mechanism by which elevated Pi promotes VSMC phenotype change is unclear.

The most abundant phosphate transporters in VSMCs are SLC20A1 (PiT-1) and SLC20A2 (PiT-2) [9]. SLC20A1 and SLC20A2 are type III sodium-dependent phosphate co-transporters that use the inward sodium gradient across the cell membrane to transport two sodium ions for every one inorganic phosphate ion into the cell [10]. These transporters are thought to play a role in intracellular Pi homeostasis as part of a balance between Pi influx and efflux [11], however, recent findings have suggested tissue-specific roles for SLC20A1 and SLC20A2 independent of their Pi uptake function [10]. SLC20A1 and SLC20A2 are now recognized as mammalian Pi sensors [12]. In VSMCs, SLC20A1 has been shown to be required for elevated Pi-induced matrix mineralization and VSMC phenotype change [9]. However, SLC20A1 is a high-affinity low-capacity transporter, and the concentration of Pi required to induce matrix mineralization is well above the concentration with maximal Pi uptake [13, 14]. In a previous study, we had shown that a Pi uptake-independent function of SLC20A1 was required for elevated Pi-induced ERK1/2 phosphorylation that leads to VSMC phenotype change [14]. These results suggested that SLC20A1-mediated Pi sensing induces a signal transduction between SLC20A1 and ERK1/2 that results in down-regulation of smooth muscle genes, but required cofactors remained unknown.

A potential adaptor protein that interacts with SLC20A1 is Rap1 guanine nucleotide exchange factor (RapGEF1). A previous study investigated protein interactions in human liver lysates by a high-throughput yeast-two-hybrid assay and identified three potential interacting partners of SLC20A1: MEK6, BCL10, and RapGEF1 [15]. Of these three proteins, RapGEF1 has been shown to have the most direct signaling connection to ERK1/2 signaling. RapGEF1 is an activator of the small GTPase Rap1 [16]. RapGEF1 is required for ERK1/2 phosphorylation in specific pathways involving Rap1 activation and down-stream B-Raf and MEK1/2 phosphorylation [16, 17]. That same cell pathway

resulted in phosphorylation of Elk-1 [17], which is a transcription factor that inhibits the smooth muscle cell promoting transcription factor, myocardin, from binding to smooth muscle-specific promoter regions and therefore inhibiting smooth muscle genes [18, 19]. Together, these data suggest that RapGEF1 may play a role in SLC20A1-mediated ERK1/2 phosphorylation and VSMC phenotype change. The research presented here tests the hypothesis that RapGEF1 is required for elevated Pi-induced ERK1/2 phosphorylation and down-regulation of smooth muscle genes.

Materials and Methods

Cell culture and maintenance

Human new-born VSMCs (HNBSMCs) used in experiments were previously published [9]. HNBSMCs were passaged and maintained in Dulbecco's Modified Eagle Medium (DMEM, Gibco Life Technologies, Cat#11995) supplemented with 15% Fetal Bovine Serum (FBS, HyClone), 1% penicillin/1% streptomycin (Life Technologies). Primary medial VSMCs were isolated from aortas of C57BL/6 mice (MVSMC) as previously described [14]. Briefly, aortas were removed from 4 –5 week-old mice, the medial layer was isolated and digested in collagen and elastin, and the primary (P0) VSMCs were incubated in DMEM supplemented with 20% FBS, 1% antibiotic/antimycotic, 1% glutamine, and 1% non-essential amino acids (Life Technologies). VSMCs were passaged and maintained in DMEM supplemented with 10% FBS and 1% antibiotic/antimycotic. Experiments used primary VSMCs between P5 and P9.

Fluorescent immunocytochemistry

Immunocytochemistry was performed by culturing either HNBSMCs or MVSMCs in normal growth media on glass slides coated with poly-D-lysine. HNBSMCs were used for PiT-1/RapGEF1 co-localization experiments and MVSMCs were used for RapGEF1 knockdown confirmation experiments. Cells were fixed with 4% paraformaldehyde and permeabilized with PBS containing 0.25% Triton-X100. Fixed cells were blocked with PBS-T containing 0.25% bovine serum albumin (BSA, Sigma-Aldrich) and 4% donkey serum (Jackson ImmunoResearch). Primary antibodies against RapGEF1 (Rabbit polyclonal IgG anti-Rapgef1 C-19, Santa Cruz Biotechnologies) or SLC20A1 (Chicken anti-SLC20A1, gift from Dr. Moshe Levi, UC Boulder) and fluorescent secondary antibodies against Rabbit IgG (Alexa 488-conjugated Donkey anti-Rabbit IgG, Jackson ImmunoResearch) or Chicken IgY (TRITC-conjugated Rabbit anti-Chicken IgY Novex, Life Technologies) were diluted in PBS-T containing 0.25% BSA and 2% donkey serum. The Chicken anti-SCL20A1 antibody has been successfully generated, validated, and used previously [13]. Antibodies were incubated in succession to avoid cross signals. Slides were mounted with Prolong Gold Anti-fade Mountant (Prolong Thermo Fisher Scientific). Imaging was performed with either a Nikon E800 Upright Microscope or a Leica SP8X Confocal Microscope at the University of Washington Keck Microscopy Facility. Image processing was performed with ImageJ Colocalization Finder and JACoP plug-ins.

RapGEF1 RNA silencing

MVSMCs were seeded at 2.5×10^4 cells per well in 6-well plates. 24 hours after seeding, siRNA directed towards RapGEF1 (Silencer Select s98950, Thermo Fisher Scientific) or non-targeting Negative control (Silencer Select 4390843, Thermo Fisher Scientific) was administered as described in the Lipofectamine RNAiMAX protocol (Life Technologies). Briefly, 5 μL of 1mM siRNA was added to 250 μL Opti-MEM (Gibco Life Technologies, Cat#31985), 1.5 μL of RNAiMAX was added to another 250 μL Opti-MEM, these dilutions were mixed and incubated for 5 minutes, VSMCs were refed with 10% FBS DMEM containing no antibiotics, and the 500 μL Opti-MEM dilution of siRNA and RNAiMAX was added to the VSMCs.

Quantitative PCR

RNA was quantified by Q-PCR. Specific genes were quantified using primers and probes directed towards RapGEF1 (TaqMan Cat#4331182, Thermo Fisher Scientific) or SM22α (forward: 5'-GACTGACATGTTCCAGACTGTTGAC-3', reverse: 5'-CAAACTGCCCAAAGCCATTAG-3', probe: FAM-5'-TGAAGGTAAGGATATGGCAGC-3'-MGB). Relative gene values were normalized to 18s ribosomal control values in each sample (Applied Biosystems), then normalized to control values using the ΔΔ18s method.

Elevated Pi-induced ERK1/2 phosphorylation assay

ERK1/2 phosphorylation assay was performed as previously described [14]. Briefly, VSMCs were incubated in Pi-free DMEM (Gibco Life Technologies Cat#11971) supplemented with 1% FBS for 16 hours, then refed with Pi-free DMEM containing different concentrations of sodium phosphate (available Pi in a buffered NaH_2PO_4 and Na_2HPO_4 solution to pH 7.4), FBS, or $NaSO_4$ (Sigma-Aldrich). Inhibitors were either added during the first Pi-free DMEM with 1% FBS refeed at 16 hours before incubation with different Pi conditions or in Pi-free DMEM with 1% FBS at 1 hour before induction with different Pi concentrations. Rap1 phosphorylation was inhibited with GGTI-298 (Sigma Aldrich), B-Raf phosphorylation was inhibited with GDC-0897 (Fisher Scientific), and Mek1/2 phosphorylation was inhibited with U0126 (Sigma Aldrich). Cells were lysed after 15 minutes in Lysate Buffer (0.1 M Tris pH = 6.8, 2% SDS) with Protease Inhibitor Cocktail (Roche), PMSF (Sigma-Aldrich), and Halt Phosphatase Inhibitor Cocktail (Thermo Scientific). Lysates were run on a western blot with antibodies against phosphorylated ERK1/2 or total ERK1/2 (Cell Signaling Technologies). Protein bands were quantified by ImageJ densitometry analysis, and phosphorylated ERK1/2 was normalized to total ERK1/2 for each sample. ERK1/2 phosphorylation was also quantified by the Thermo Scientific Pierce ERK1/2 Colorimetric In-Cell ELISA Kit (Thermo Fisher). VSMCs were seeded in 96-well plates in growth media, refed with Pi-free DMEM with 1% FBS and incubated for 16 hours, refed with Pi-free DMEM with 1% FBS with added inhibitor and incubated for 1 hour, then refed with Pi-free DMEM containing added inhibitor and different concentrations of Pi, FBS, or $NaSO_4$. Cells were fixed with 4% paraformaldehyde at various times after incubation, and the In-Cell ELISA Kit protocol was followed to obtain absorbance readings corresponding to amount of phosphorylated ERK1/2.

Statistical Analysis

GraphPad Prism 8 software (San Diego, CA) was used to perform statistical tests (two-way ANOVA followed by Sidak's multiple comparison test, one-way ANOVA followed by Tukey's multiple comparison test, or unpaired t-test). A p-value of less than 0.05 was considered statistically significant. Statistical significance of fluorescence overlap was determined by ImageJ software analysis using Manders Overlap Coefficient determination.

Results

RapGEF1 and SLC20A1 proteins co-localize in VSMCs

A previously published study identified SLC20A1 and RapGEF1 as potential binding partners in a yeast-two-hybrid assay [15], suggesting that these proteins might associate in a signaling complex, but confirmation in mammalian cells was not performed. To investigate whether SLC20A1 and RapGEF1 might be part of a signaling complex in VSMCs, fluorescent immunocytochemistry was performed and imaged by confocal microscopy to determine colocalization. Immortalized human VSMCs (HNBSMCs) were used in this experiment because the available antibodies were raised against human peptide segments. Both SLC20A1 and RapGEF1 were expressed in cultured HNBSMCs with similar peri-membranous and cytosolic localization patterns (Fig. 1A-B). An overlay of SLC20A1, RapGEF1, and DAPI staining showed co-localization throughout the cell (Fig. 1C). Co-localization of SLC20A1 and RapGEF1 staining was processed and visualized (Fig. 1D). Manders Overlap Coefficients (similar to R values in linear regression analysis) were determined to be 0.788 for SLC20A1 co-staining with RapGEF1 and 0.612 for RapGEF1 co-staining with SLC20A1, showing that SLC20A1 and RapGEF1 protein have a large degree of co-localization.

RNA silencing of RapGEF1 eliminates elevated Pi-induced ERK1/2 phosphorylation

Pi uptake-independent function of SLC20A1 is required for elevated Pi-induced ERK1/2 phosphorylation in VSMCs [14]. To investigate the role of RapGEF1 in elevated Pi -induced ERK1/2 phosphorylation, small interfering RNA was used to silence RapGEF1 mRNA (siRapGEF1), and the effect of elevated Pi on phosphorylated ERK1/2 was assessed. Primary murine VSMCs (MVSMCs) were used in these experiments instead of the immortalized HNBSMC lines because primary cells have more physiologically-relevant cell signaling responses. MVSMCs transfected with siRapGEF1 showed a greater than 95% reduction in RapGEF1 mRNA compared to negative control siRNA (siNegative) at 2, 3, and 4 days after siRNA transfection (Fig. 2A). Protein reduction was also visible through fluorescent immunocytochemistry of RapGEF1 protein in siNegative and siRapGEF1 MVSMCs (Fig. 2B-C), and fluorescent intensity was decreased by 67% (Fig. 2D). ERK1/2 phosphorylation was visualized by western blot in siNegative and siRapGEF1 MVSMCs after induction with either 0.5mM, 1.0mM, or 3.0mM Pi (Fig. 2E). Densitometry quantification showed that ERK1/2 phosphorylation in siNegative MVSMCs was increased 1.5-fold in 3.0mM Pi media over 1.0mM Pi media, but RapGEF1 siRNA eliminated this effect (Fig. 2F). Together, these data show that silencing RapGEF1 mRNA and protein eliminates the elevated Pi-induced increase in ERK1/2 phosphorylation in VSMCs.

Inhibition of Rap1, B-Raf, or Mek1/2 eliminates elevated Pi-induced ERK1/2 phosphorylation

Downstream of RapGEF1, Rap1 activation has been shown to promote ERK1/2 phosphorylation through a Rap1/B-Raf/Mek1/2/Erk1/2 cell signaling cascade in other cell types [17]. To test the importance of these intermediate proteins in RapGEF1-mediated cell signaling to ERK1/2, phosphorylation of each intermediate protein was pharmacologically inhibited, and elevated Pi-induced ERK1/2 phosphorylation was assessed. Specific small molecule inhibitors have been generated that block activation of Rap1, B-Raf, and Mek1/2 individually (GGTI-298, GDC-0879, and U0126, respectively) (Fig. 3A). MVSMCs were incubated in Pi-free DMEM with serial dilutions each inhibitor (starting at 20μM GGTI298, 10μM GDC0879, and 20μM U0126) or 0.5% DMSO control for 16 hours before elevated Pi induction. Western blot of P-ERK1/2 for each condition showed that 3.0mM Pi induced ERK1/2 phosphorylation in the control treatment, but the highest concentrations of each inhibitor all blocked ERK1/2 phosphorylation (Fig. 3B). As the inhibitor was diluted, ERK1/2 phosphorylation increased to resemble the 3.0mM Pi control induction. Then, we further investigated the largest concentration of each inhibitor with a 1-hour pre-incubation before elevated Pi induction. Western blot of P-ERK1/2 and total ERK1/2 showed that ERK1/2 phosphorylation was reduced in all of the inhibitor cases compared 3.0mM Pi induction in control treated VSMCs (Fig. 3C). Additionally, induction of ERK1/2 phosphorylation was more accurately quantified by In-Cell ERK1/2 ELISA assay, which confirmed that small molecule inhibitor treatment significantly completely blocked the increase in ERK1/2 phosphorylation that was observed in the DMSO control samples (Fig. 3D). Together, these results show that Rap1, B-Raf, and Mek1/2 are all involved in elevated Pi-induced ERK1/2 phosphorylation in VSMCs, suggesting that the Rap1/B-Raf/Mek1/2 signaling axis is down-stream of RapGEF1-mediated cell signaling in response to elevated Pi.

RNA silencing of RapGEF1 transiently up-regulates SM22α and eliminates elevated Pi-induced down-regulation of SM22α

Down-stream of ERK1/2 phosphorylation, SLC20A1-mediated cell signaling inhibits SM22α expression in VSMCs consistent with VSMC phenotype change [14]. Therefore, changes in SM22α mRNA expression were investigated with RapGEF1 siRNA to assess the role of RapGEF1 in VSMC phenotype change. First, SM22α mRNA expression was quantified in normal growth media in MVSMCs treated with siNegative control or siRapGEF1. SM22α mRNA expression was increased by 5-fold after 2 days of siRNA treatment and by 9-fold after 3 days of siRNA treatment, but was reduced to control levels by day 4 (Fig. 4A). This showed that siRNA knockdown of RapGEF1 resulted in a transient up-regulation of SM22α mRNA expression that was normalized by 4 days post-siRNA treatment. Next, the role of RapGEF1 in SM22α mRNA inhibition by elevated Pi was assessed. SM22α mRNA expression was reduced in siNegative MVSMCs after 4 days of elevated Pi treatment compared to normal Pi conditions, but siRapGEF1 showed no SM22α reduction in elevated Pi treatment (Fig. 4B). Therefore, RapGEF1 was required for inhibition of SM22α mRNA expression both transiently in normal media and in response to elevated Pi induction.

Discussion

The results presented here suggest that RapGEF1 co-localizes with SLC20A1 in VSMCs, and that ERK1/2 cell signaling and VSMC phenotype change in response to elevated Pi requires RapGEF1. This signaling pathway goes through a Rap1/B-Raf/Mek1/2 cascade. Overall, the data suggest that elevated Pi initiates formation of a protein complex that may contain both SLC20A1 and RapGEF1, and requires Rap1, B-Raf, and Mek1/2 to phosphorylate ERK1/2 and down-regulate smooth muscle-specific genes.

RapGEF1 has several known functions and mechanisms of activation. In mice, global deletion of RapGEF1 is embryonically lethal at E7.5 due to decreased cell adhesion of embryonic fibroblasts and decreased embryogenesis [20]. Other studies have also implicated RapGEF1-meditated activation of Rap1 on cell adhesion function and ERK1/2 phosphorylation [17, 21, 22]. Most interesting to the results of this study, RapGEF1 was found to be required for vascular maturation of embryos [23]. That study found that transgenic mice hypomorphic for RapGEF1 died in embryo at age E11.5 due to vascular integrity defects, which is a strikingly similar phenotype to the SLC20A1 global deletion mouse that is embryonically lethal at E14.5 and had vascular defects starting at E11.5 [24]. The signaling pathway and down-stream regulation of smooth muscle cell genes presented in the results may help explain the role of RapGEF1 in vascular maturation.

RapGEF1 localization also seems to play a large role in the activation of Rap1 and down-stream signaling proteins. A membrane localization signal attached to RapGEF1 was sufficient to activate Rap1 [16]. Furthermore, a previous study found that although Epac1 (a different Rap1 activator) does not normally lead to ERK1/2 phosphorylation, adding a membrane localization signal to Epac1 does lead to down-stream ERK1/2 phosphorylation after Rap1 activation [25]. Membrane localization of RapGEF1 could be the initiation mechanism for the cell signaling response to elevated Pi. RapGEF1 binding to SLC20A1 on the cell membrane may be enough to initiate the cell signaling response to elevated Pi through ERK1/2 phosphorylation. This underlying mechanism could also suggest a role for SLC20A1 and RapGEF1 signaling in mammalian cell Pi sensing, although this hypothesis needs to be tested *in vivo* and in many different cell types.

Whether SLC20A1 binds directly to RapGEF1 within peri-membranous complexes is not yet known. Lack of immunoprecipitation-competent SLC20A1 or RapGEF1 antibodies hindered our ability to use this method to confirm a direct protein-protein interaction (data not shown). However, SLC20A1 has been recently found to form complexes with other proteins. Bon et al. showed that SLC20A1 forms a heterodimer with the related family member, SLC20A2. This complex has been implicated in extracellular Pi sensing independent of Pi transport in bone [26]. The mechanism of RapGEF1 interaction with the SLC20A1-mediated extracellular Pi response pathway may be complex, involving multiple proteins, intracellular localization, and/or several downstream signaling responses. Future experiments need to be performed to elucidate this complicated mechanism involving SLC20A1 and RapGEF1 interactions.

This signaling pathway initiated by elevated Pi, induced through SLC20A1 and RapGEF1, and leads to inhibition of VSMC-specific genes could be important in vascular disease phenotypes. VSMCs are plastic and have the ability to transdifferentiate into different phenotypes depending on the extracellular stimuli [27]. VSMC phenotype change can lead to proliferative, migratory, ECM degrading, or calcifying VSMCs that are present in vascular diseases such as atherosclerosis, restenosis, and vascular calcification [27]. Inhibition of VSMC gene s, such as SM22α, is one of the first steps in VSMC transdifferentiation, suggesting that this signaling pathway initiated by SLC20A1 binding to RapGEF1 and leads to ERK1/2 phosphorylation may play an important role in VSMC phenotype change in vascular disease [28]. Further *in vivo* studies with models of specific vascular diseases are necessary to test these hypotheses.

Other developmental and tissue maintenance processes that require SLC20A1 and proper Pi handling may also require this signaling pathway. SLC20A1 was found to be essential for skeletal development through promoting chondrocyte survival, and these functions were independent of Pi uptake [29]. In osteoblasts, extracellular Pi promotes ERK1/2 phosphorylation and expression of Dmp1 through SLC20A1 [30]. Additionally, Chande et al. found that postnatal deletion of SLC20A1 and SLC20A2 in mouse skeletal muscle resulted in muscle atrophy with reduced ERK1/2 phosphorylation [31]. These studies linking SLC20A1 to ERK1/2 phosphorylation in multiple cell types suggest that this pathway may be important in other processes as well.

In conclusion, the data presented here suggest that RapGEF1 is required for the SLC20A1-mediated elevated Pi signaling pathway through Rap1, B-Raf, and Mek1/2 to increase ERK1/2 phosphorylation and inhibit smooth muscle cell gene expression in VSMCs.

Acknowledgements

The authors acknowledge the W. M. Keck Microscopy Center and director Dr. Nathaniel Peters for confocal fluorescence imaging training and equipment access, performed on the Leica SP8X confocal microscope (funded by NIH S10 OD016240 and UW Student Technology Fee).

Funding Sources

This study was supported by grants to N.W.C. (NIH T32 EB001650) and C.M.G. (NIH R35 HL139602).

Bibliography

1. LeGeros RZ. Formation and transformation of calcium phosphates: relevance to vascular calcification. Z Kardiol. 2001;90 Suppl 3:116–24. [PubMed: 11374023]
2. Shanahan CM, Crouthamel MH, Kapustin A, Giachelli CM. Arterial calcification in chronic kidney disease: key roles for calcium and phosphate. Circ Res. 20119;109(6):697–711. [PubMed: 21885837]
3. Goretti Penido M, Alon US. Phosphate homeostasis and its role in bone health. Pediatr Nephrol. 2012 11;27(11):2039–48. [PubMed: 22552885]
4. Block GA, Hulbert-Shearon TE, Levin NW, Port FK. Association of serum phosphorus and calcium x phosphate product with mortality risk in chronic hemodialysis patients: a national study. Am J Kidney Dis. 19984;31(4):607–17. [PubMed: 9531176]
5. Tonelli M, Sacks F, Pfeffer M, Gao Z, Curhan G, Investigators CARET. Relation between serum phosphate level and cardiovascular event rate in people with coronary disease. Circulation. 200510;112(17):2627–33. [PubMed: 16246962]

6. Adeney KL, Siscovick DS, Ix JH, Seliger SL, Shlipak MG, Jenny NS, et al.Association of serum phosphate with vascular and valvular calcification in moderate CKD. J Am Soc Nephrol. 20092;20(2):381–7. [PubMed: 19073826]
7. Speer MY, Yang HY, Brabb T, Leaf E, Look A, Lin WL, et al.Smooth muscle cells give rise to osteochondrogenic precursors and chondrocytes in calcifying arteries. Circ Res. 20093;104(6):733–41. [PubMed: 19197075]
8. Speer MY, Li X, Hiremath PG, Giachelli CM. Runx2/Cbfa1, but not loss of myocardin, is required for smooth muscle cell lineage reprogramming toward osteochondrogenesis. J Cell Biochem. 20107;110(4):935–47. [PubMed: 20564193]
9. Li X, Yang HY, Giachelli CM. Role of the sodium-dependent phosphate cotransporter, Pit-1, in vascular smooth muscle cell calcification. Circ Res. 20064;98(7):905–12. [PubMed: 16527991]
10. Virkki LV, Biber J, Murer H, Forster IC. Phosphate transporters: a tale of two solute carrier families. Am J Physiol Renal Physiol. 20079;293(3):F643–54. [PubMed: 17581921]
11. Hortells L, Guillén N, Sosa C, Sorribas V. Several phosphate transport processes are present in vascular smooth muscle cells. Am J Physiol Heart Circ Physiol. 202002;318(2):H448–H60. [PubMed: 31886722]
12. Beck L, Beck-Cormier S. Extracellular phosphate sensing in mammals: what do we know?J Mol Endocrinol. 202010;65(3):R53–R63. [PubMed: 32755995]
13. Villa-Bellosta R, Levi M, Sorribas V. Vascular smooth muscle cell calcification and SLC20 inorganic phosphate transporters: effects of PDGF, TNF-alpha, and Pi. Pflugers Arch. 200910;458(6):1151–61. [PubMed: 19506901]
14. Chavkin NW, Chia JJ, Crouthamel MH, Giachelli CM. Phosphate uptake-independent signaling functions of the type III sodium-dependent phosphate transporter, PiT-1, in vascular smooth muscle cells. Exp Cell Res. 20154;333(1):39–48. [PubMed: 25684711]
15. Wang J, Huo K, Ma L, Tang L, Li D, Huang X, et al.Toward an understanding of the protein interaction network of the human liver. Mol Syst Biol. 201110;7:536. [PubMed: 21988832]
16. Gotoh T, Hattori S, Nakamura S, Kitayama H, Noda M, Takai Y, et al.Identification of Rap1 as a target for the Crk SH3 domain-binding guanine nucleotide-releasing factor C3G. Mol Cell Biol. 199512;15(12):6746–53. [PubMed: 8524240]
17. Vossler MR, Yao H, York RD, Pan MG, Rim CS, Stork PJ. cAMP activates MAP kinase and Elk-1 through a B-Raf- and Rap1-dependent pathway. Cell. 19974;89(1):73–82. [PubMed: 9094716]
18. Yoshida T, Sinha S, Dandré F, Wamhoff BR, Hoofnagle MH, Kremer BE, et al.Myocardin is a key regulator of CArG-dependent transcription of multiple smooth muscle marker genes. Circ Res. 20035;92(8):856–64. [PubMed: 12663482]
19. Kawai-Kowase K, Owens GK. Multiple repressor pathways contribute to phenotypic switching of vascular smooth muscle cells. Am J Physiol Cell Physiol. 20071;292(1):C59–69. [PubMed: 16956962]
20. Ohba Y, Ikuta K, Ogura A, Matsuda J, Mochizuki N, Nagashima K, et al.Requirement for C3G-dependent Rap1 activation for cell adhesion and embryogenesis. EMBO J. 20017;20(13):3333–41. [PubMed: 11432821]
21. Arai A, Nosaka Y, Kohsaka H, Miyasaka N, Miura O. CrkL activates integrin-mediated hematopoietic cell adhesion through the guanine nucleotide exchange factor C3G. Blood. 19996;93(11):3713–22. [PubMed: 10339478]
22. Bos JL. Linking Rap to cell adhesion. Curr Opin Cell Biol. 20054;17(2):123–8. [PubMed: 15780587]
23. Voss AK, Gruss P, Thomas T. The guanine nucleotide exchange factor C3G is necessary for the formation of focal adhesions and vascular maturation. Development. 20031;130(2):355–67. [PubMed: 12466202]
24. Festing MH, Speer MY, Yang HY, Giachelli CM. Generation of mouse conditional and null alleles of the type III sodium-dependent phosphate cotransporter PiT-1. Genesis. 200912;47(12):858–63. [PubMed: 19882669]
25. Wang Z, Dillon TJ, Pokala V, Mishra S, Labudda K, Hunter B, et al.Rap1-mediated activation of extracellular signal-regulated kinases by cyclic AMP is dependent on the mode of Rap1 activation. Mol Cell Biol. 20063;26(6):2130–45. [PubMed: 16507992]

26. Bon N, Couasnay G, Bourgine A, Sourice S, Beck-Cormier S, Guicheux J, et al.Phosphate (P(i))-regulated heterodimerization of the high-affinity sodium-dependent P(i) transporters PiT1/Slc20a1 and PiT-2/Slc20a2 underlies extracellular P(i) sensing independently of P(i) uptake. J Biol Chem. 201802;293(6):2102–14. [PubMed: 29233890]

27. Alexander MR, Owens GK. Epigenetic control of smooth muscle cell differentiation and phenotypic switching in vascular development and disease. Annu Rev Physiol. 2012;74:13–40. [PubMed: 22017177]

28. Hendrix JA, Wamhoff BR, McDonald OG, Sinha S, Yoshida T, Owens GK. 5' CArG degeneracy in smooth muscle alpha-actin is required for injury-induced gene suppression in vivo. J Clin Invest. 20052;115(2):418–27. [PubMed: 15690088]

29. Couasnay G, Bon N, Devignes CS, Sourice S, Bianchi A, Véziers J, et al.PiT1/Slc20a1 Is Required for Endoplasmic Reticulum Homeostasis, Chondrocyte Survival, and Skeletal Development. J Bone Miner Res. 2019 02;34(2):387–98. [PubMed: 30347511]

30. Nishino J, Yamazaki M, Kawai M, Tachikawa K, Yamamoto K, Miyagawa K, et al.Extracellular Phosphate Induces the Expression of Dentin Matrix Protein 1 Through the FGF Receptor in Osteoblasts. J Cell Biochem. 201705;118(5):1151–63. [PubMed: 27639037]

31. Chande S, Caballero D, Ho BB, Fetene J, Serna J, Pesta D, et al.Slc20a1/Pit1 and Slc20a2/Pit2 are essential for normal skeletal myofiber function and survival. Sci Rep. 202002;10(1):3069. [PubMed: 32080237]

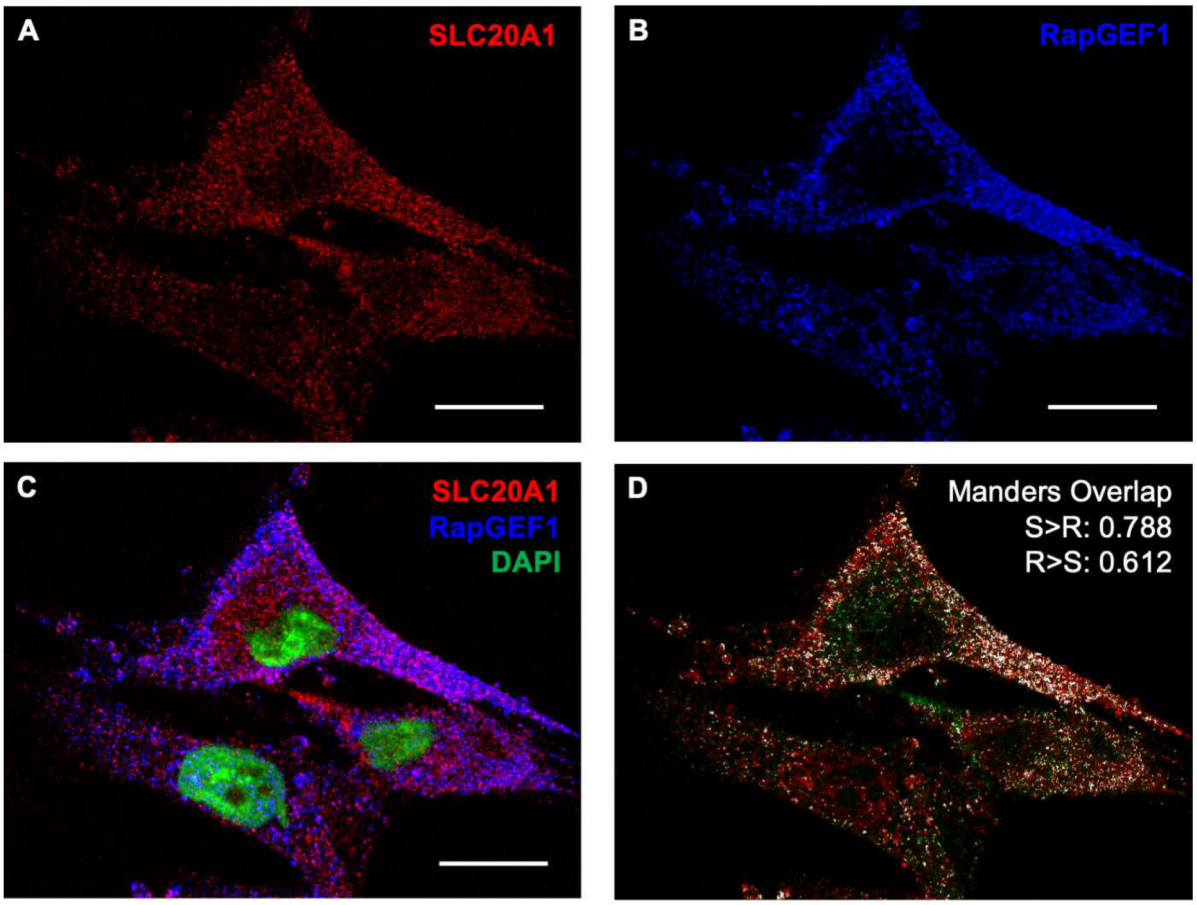

Figure 1. Visualization and quantification of SLC20A1 and RapGEF1.

Fluorescent immunocytochemistry of cultured HNBSMCs in normal Pi concentration (1.0 mM) probing for A) SLC20A1 (Red) and B) RapGEF1 (Blue) (scale bars = 20μm). C) An overlay was performed showing DAPI (Green) and co-staining between SLC20A1 and RapGEF1 (Purple). D) ImageJ analysis highlights co-localization of staining, with Manders Overlap Coefficients calculated for SLC20A1 on RapGEF1 (S>R) and RapGEF1 on SLC20A1 (R>S) (Co-staining in White).

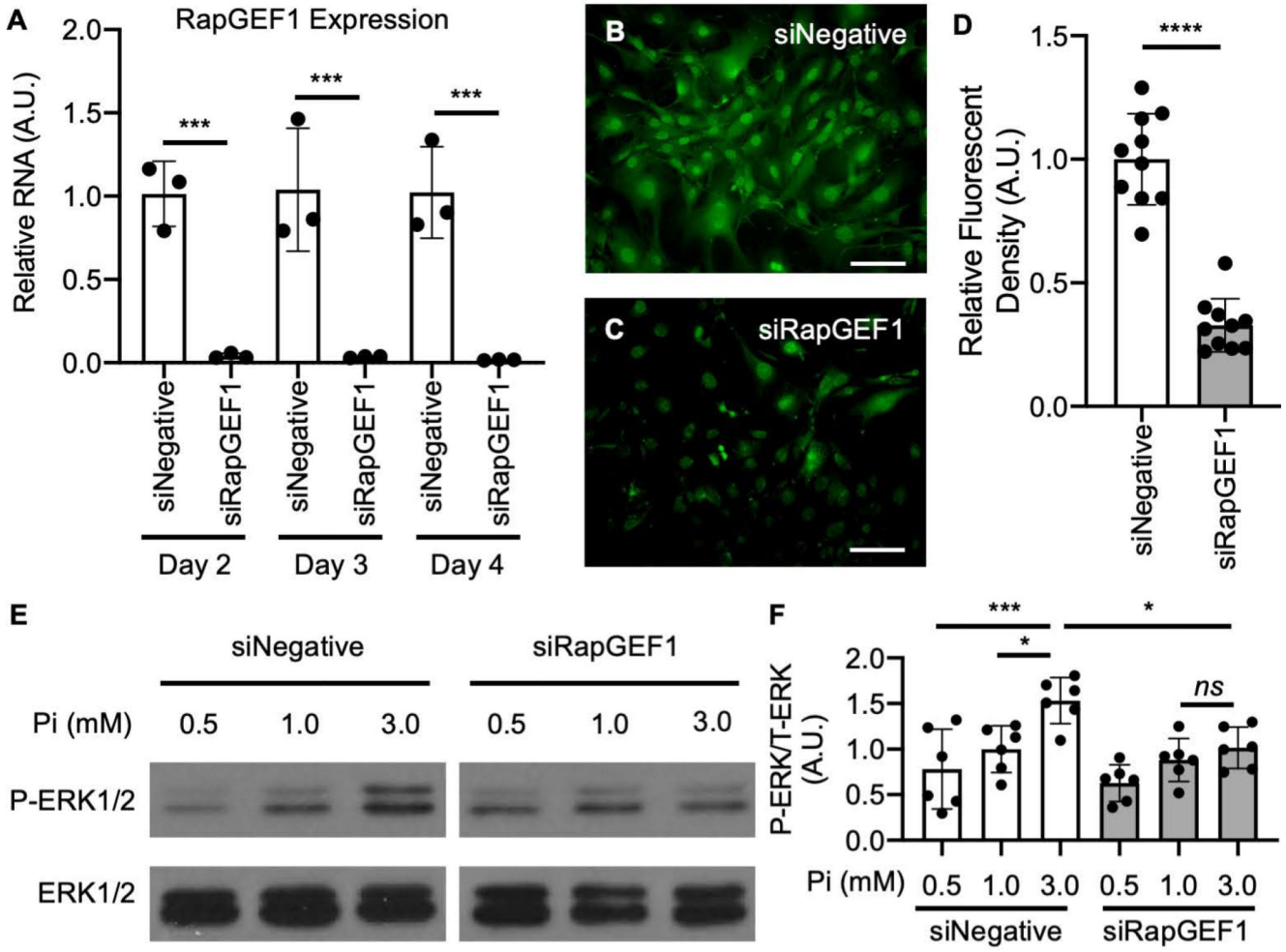

Figure 2. RapGEF1 silencing eliminates elevated Pi-induced ERK1/2 phosphorylation.

Primary murine VSMCs were transfected with either RapGEF1 siRNA (siRapGEF1) or negative control siRNA (siNegative). A) RapGEF1 RNA was quantified with qRT-PCR on day 2, 3, and 4 after siRNA transfection. Immunocytochemistry probing for RapGEF1 (green) and was used to visualize RapGEF1 protein in B) siNegative and C) siRapGEF1 VSMCs (scale bar = 100μm). D) 10 cells/image were quantified for total cell fluorescence to show RapGEF1 protein depletion in siRNA treated VSMCs. E) Both siNegative and siRapGEF1 VSMCs were incubated in media containing either 0.5mM, 1.0mM, or 3.0mM Pi for 15 minutes ERK1/2 phosphorylation was visualized by western blot (representative image shown). F) Quantification of six independent samples was performed by densitometry analysis. (two-way ANOVA post-hoc Sidak in A, student's t-test in D, one-way ANOVA post-hoc Tukey in F: *ns* = $p > 0.05$, * = $p < 0.05$, ** = $p < 0.01$, *** = $p < 0.001$, **** = $p < 0.0001$)

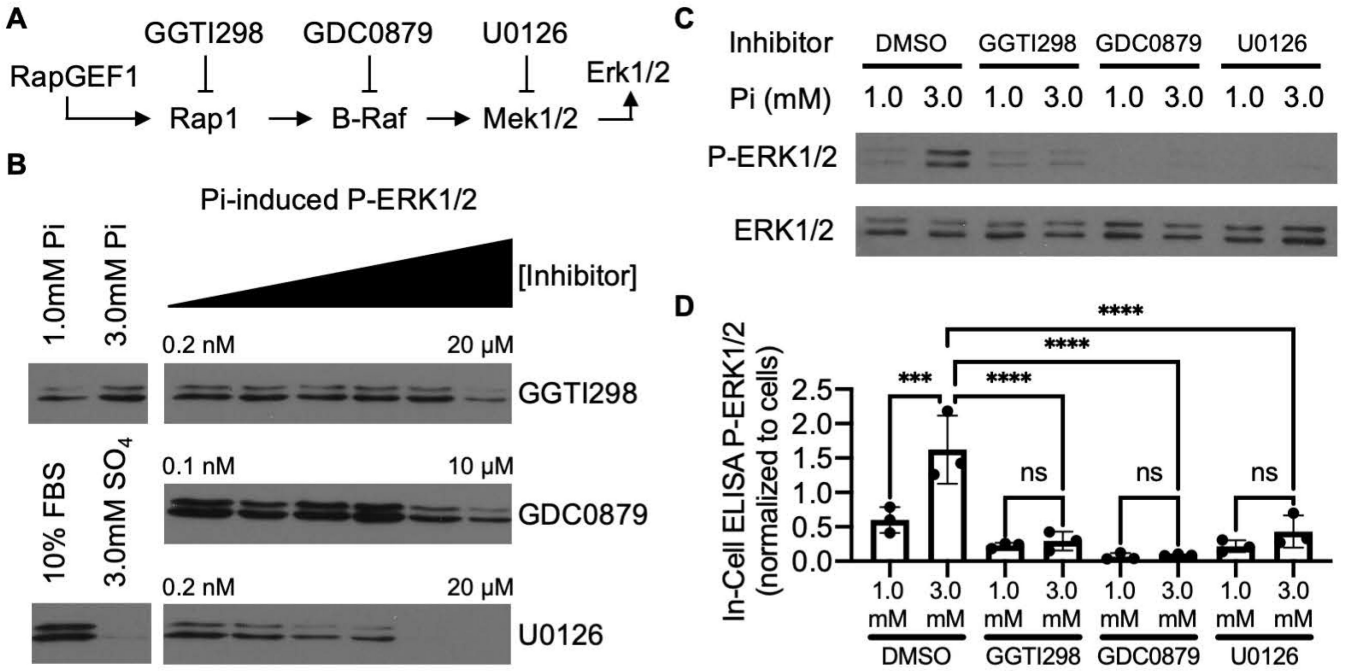

Figure 3. Inhibitors against Rap1, B-Raf, and Mek1/2 eliminate elevated Pi-induced ERK1/2 phosphorylation.

Elevated Pi -induced ERK1/2 phosphorylation was assessed with small molecule inhibitors against Rap1 (GGTI298), B-Raf (GDC0879), and Mek1/2 (U0126). A) Schematic represents the effects of each small molecule inhibitor on proteins involved in the signaling pathway. B) Primary murine VSMCs were incubated in Pi-free DMEM with varying inhibitor concentrations for 16 hours starting at 20μM GGTI298, 10μM GDC0879, or 20μM U0126 and diluted serially with a dilution factor of 10, then induced with 3.0mM Pi (or given controls), and phosphorylated ERK1/2 was quantified by western blot. C) VSMCs were incubated in Pi-free DMEM overnight, then Pi-free DMEM with varying concentrations of inhibitors (20μM GGTI298, 10μM GDC0879, or 20μM U0126) for 1 hour, and induced with either 1.0mM or 3.0mM Pi, then ERK1/2 was visualized by western blot. D) Induction of P-ERK1/2 after pre-incubation with inhibitors and induction with 1.0mM Pi or 3.0mM Pi was quantified by In-Cell ELISA assay. (two-way ANOVA post-hoc Sidak in D: *ns* = p > 0.05, * = p < 0.05, ** = p < 0.01, *** = p < 0.001, **** = p < 0.0001)

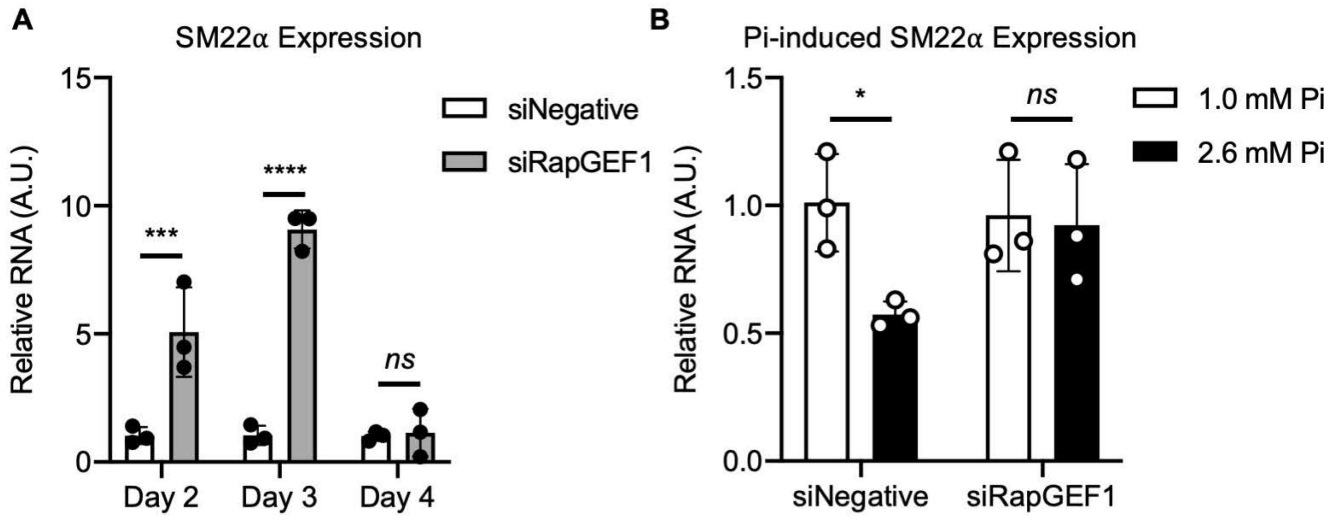

Figure 4. RapGEF1 silencing increases SM22α mRNA and eliminates elevated Pi-induced SM22α mRNA inhibition.

A) SM22α mRNA expression was quantified at day 2, 3, and 4 post-transfection with either siNegative or siRapGEF1. B) VSMCs were treated with either siNegative or siRapGEF1 and incubated for 4 days in 1.0mM Pi or 2.6mM Pi media and SM22α mRNA was quantified. (two-way ANOVA post-hoc Sidak in A and B: *ns* = $p > 0.05$, * = $p < 0.05$, ** = $p < 0.01$, *** = $p < 0.001$, **** = $p < 0.0001$)